Optical properties of (1-x)Pb(Mg13Nb23)O3-xPbTiO3 single crystals studied by spectroscopic ellipsometry

Xinming Wan, H. L. W. Chan, C. L. Choy, Xiangyong Zhao, and Haosu Luo

Citation: J. Appl. Phys. **96**, 1387 (2004); doi: 10.1063/1.1767287
View online: http://dx.doi.org/10.1063/1.1767287
View Table of Contents: http://jap.aip.org/resource/1/JAPIAU/v96/i3
Published by the American Institute of Physics.

Optical properties of $(1-x)Pb(Mg_{1/3}Nb_{2/3})O_3$-$xPbTiO_3$ single crystals studied by spectroscopic ellipsometry

Xinming Wan[a)]
Department of Applied Physics, The Hong Kong Polytechnic University Hung Hom, Hong Kong, China
The State Key Laboratory of High Performance Ceramics and Superfine Microstructure, Shanghai Institute of Ceramics, Chinese Academy of Sciences, Jiading, Shanghai 201800, China

H. L. W. Chan and C. L. Choy
Department of Applied Physics, The Hong Kong Polytechnic University Hung Hom, Hong Kong, China

Xiangyong Zhao and Haosu Luo
The State Key Laboratory of High Performance Ceramics and Superfine Microstructure, Shanghai Institute of Ceramics, Chinese Academy of Sciences Jiading, Shanghai 201800, China

(Received 8 March 2004; accepted 7 May 2004)

$(1-x)Pb(Mg_{1/3}Nb_{2/3})O_3$-$xPbTiO_3$ (PMN-x PT) single crystals with $x=0.24$, 0.30, 0.31, and 0.33 have been investigated by spectroscopic ellipsometry. The refractive indices and extinction coefficients were obtained. The modified Sellmeier equations for the refractive indices were obtained by least-squares fit. The equations can be used to calculate the refractive index with high accuracy in the low absorption wavelength range, namely, from 400 to 5800 nm. The Sellmeier optical coefficients E_0, λ_0, S_0, and E_d were calculated by fitting the single-term oscillator equation. They are related directly to the electronic energy band structure and have the physical significance. The optical band gap energies were also obtained from absorption coefficient spectra. Our results show that as the PT content increases, the refractive index of PMN-xPT single crystals increases, while the optical band gap energy decreases. Some discussions about the BO_6 octahedron building block that determines the basic energy level of PMN-xPT single crystals are also presented in this article. © *2004 American Institute of Physics*. [DOI: 10.1063/1.1767287]

I. INTRODUCTION

The complex perovskite $(1-x)Pb(Mg_{1/3}Nb_{2/3})O_3$-$xPbTiO_3$ (PMN-x PT) single crystals are well-known ferroelectrics with an ABO_3-type oxygen-octahedral unit cell. They have come into prominence due to their extrahigh electromechanical coupling factor, piezoelectric and dielectric coefficients, and field induced strain response.[1–3] Most oxygen-octahedral ferroelectrics, which exhibit excellent electromechanical properties, also have outstanding optical properties.[4,5] Although lots of work on the dielectric and piezoelectric properties of PMN-xPT single crystals have been done, the values of the optical properties are not perfectly known. The knowledge of the detailed optical parameters, such as the refractive indices or optical transmission properties, is most desirable, not only for making possible practical usage in optic devices but also to answer very basic questions on the energy level of the crystals and the physical nature of this class of relaxor ferroelectrics.

One of the most important factors determining the use of a new-style material for optical applications is its refractive index n and extinction coefficient k. Studies have been reported on the refractive indices of PMN single crystal,[6] PMN-0.3PT ceramics,[7] PMN-0.38PT single crystal,[8,9] and $PbTiO_3$ ceramics.[10] The values are 2.522, 2.598, 2.620, and 2.668 at 633 nm, respectively. Bing, Guo, and Bhalla further suggested that for the PMN-xPT family, the refractive indices increase with PT content.[7] But the dependence of the refractive indices as well as extinction coefficients of PMN-xPT single crystals as a function of PT content is largely unknown. The lack of experimental data is mainly due to the difficulties of applying traditional Brewster's angle or minimum deviation method to small single crystals with poor optical quality. PMN-xPT single crystals of $x<0.35$ have many domain walls and nanoregions with different orientation which obviously cause multiple scattering and generate large scattering losses, so they become opaque when the thickness is over 1 mm. These limitations are known to be avoidable by using spectroscopic ellipsometry (SE).[11,12] SE is a nondestructive and powerful technique to investigate the optical characteristics of both bulk materials and thin films.

The aim of this article is to provide a complete set of data of the refractive indices and extinction coefficients for PMN-xPT single crystals. We measured the ellipsometric spectra of four typical samples with $x=0.24$, 0.30, 0.31, and 0.33. Their Sellmeier equations for the refractive indices were obtained in terms of least-squares fit. The Sellmeier optical coefficients E_0, λ_0, S_0, and E_d were also calculated through fitting the single-term oscillator equation. From the extinction coefficient spectra, the absorption coefficient spectra, and hence the optical band gap energies of PMN-xPT single crystals were estimated.

II. EXPERIMENTAL PROCEDURE

The ferroelectric PMN-xPT single crystals were grown directly from melt by the modified Bridgman technique.[2,13]

[a)]Electronic mail: xmwan@citiz.net

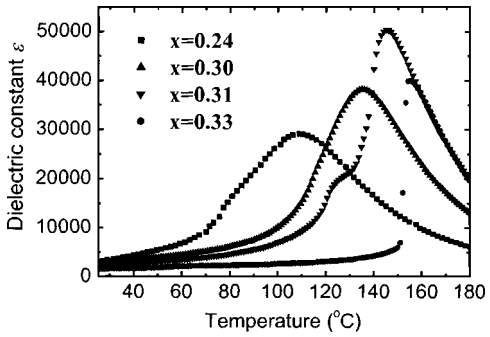

FIG. 1. Temperature dependence of dielectric constants at 1 kHz of PMN -*x*PT single crystals.

For unpoled PMN-*x*PT single crystals with $x<0.33$, they retain an optical isotropic pseudocubic state. That is to say, *a*, *b* and *c* axes are almost the same. In this work, all the samples were oriented and cut along the ⟨001⟩ direction using an x-ray diffractometer. Our experimental samples are 5×5 mm^2 square slabs with thickness of 1 mm. As the segregation behavior during the crystal growth results in the variation of PT content along the same boule,[14] we should determine *x*, the PT content firstly. For PMN-*x*PT single crystals, *x* can be estimated by T_m, which approximately equals to the Curie temperature T_c.[15] In this work, silver paste was painted on the sample surfaces and sintered at 580 °C for 30 min. Using an HP4194A impedance analyzer equipped with a temperature chamber (Delta 9023), the dielectric constants were measured at 1 kHz from room temperature to 180 °C and T_m was determined from the maximum of dielectric constants.

The square surfaces for light reflection were polished using alumina and diamond polishing compounds (with decreasing average grit size down to 0.05 μm) to achieve a final optical polish, with specular reflection. SE measurements were carried out at room temperature in the wavelength range of 350–820 nm with 5 nm intervals using a spectroscopic phase-modulated ellipsometer (Jobin YVON UVISEL). An incidence angle of 70° was used throughout the SE measurements.

III. RESULTS AND DISCUSSION

A. Dielectric constant versus temperature

We have prepared a series of PMN-*x*PT single crystals with different starting compounds and measured many samples. In PMN-*x*PT single crystals, the Curie temperature T_c is sensitive to the content of PT, thus we can select samples with different PT contents by measurement of their T_c in our experiment. The four selected samples with typical PT contents as representatives were reported here. Figure 1 shows the temperature dependence of the dielectric constants for the samples at the frequency of 1 kHz. The dielectric constant peaks are found at 110, 140, 145, and 155 °C, respectively. With the phase diagram of the PMN-*x*PT solid solution system and the equation published before,[15] we know that the corresponding *x* of these samples is 0.24, 0.30, 0.31, and 0.33, respectively. Many authors have reported the dielectric performance of PMN-*x*PT single crystals. The values of the dielectric constants reported for samples used in this work agree well with those reported by others.[2,16]

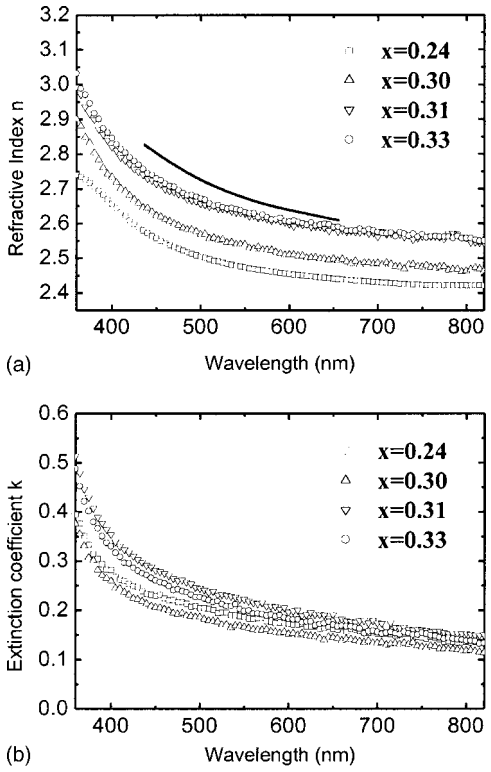

FIG. 2. Wavelength dependence of (a) the refractive indices, and (b) extinction coefficients at room temperature of PMN-*x*PT single crystals. The solid line showing the refractive index of PMN-0.38PT single crystal is obtained from Ref. 8.

B. The refractive index and extinction coefficient

SE is a very powerful technique to measure the refractive index and extinction coefficient of a wide variety of materials. In SE, one deals with the measurements of the relative changes in the amplitude and the phase of a linearly polarized monochromatic incident light upon reflection from the sample surface. The experimental quantities measured by ellipsometry are the angles Ψ and Δ, which are related to the optical and structural properties of the samples, as defined by

$$\rho = \tan\Psi e^{i\Delta} = \frac{R_p}{R_s} = \left|\frac{R_p}{R_s}\right| \exp[i(\delta_p - \delta_s)], \tag{1}$$

where the complex Fresnel reflection coefficients R_p and R_s correspond to the parallel and perpendicular components, respectively. They are complex functions of the refractive index *n* and extinction coefficient *k*. For bulk isotropic samples investigated here, their complex refractive index ($\tilde{n}=n+ik$) can be revealed automatically by comparing the computer modeling data with the experimental data.

Figure 2 depicts the wavelength dependence of the refractive indices and extinction coefficients at room temperature of PMN-*x*PT single crystals. The refractive indices decrease dramatically when the wavelength increases for all the samples. The refractive index of PMN-0.38PT single crystal measured with minimum deviation method in previous work[8] is also plotted in Fig. 2(a) for comparison. The dispersion

TABLE I. The refractive index parameters for PMN-*x*PT single crystals at room temperature.

	A	*B*	*C*	*D*
PMN–0.24 PT	5.6875	0.0924	0.0938	0.0217
PMN–0.30 PT	5.5957	0.1628	0.0686	−0.4040
PMN–0.31 PT	6.6344	0.0880	0.0979	0.6123
PMN–0.33 PT	5.9302	0.2126	0.0572	−0.4268

TABLE II. The refractive indices at 633 nm wavelength and optical band gap energies of PMN-*x*PT single crystals.

	n	E_g(nm)	E_g(eV)
PMN–0.24 PT	2.446	383.8	3.24
PMN–0.30 PT	2.501	385.1	3.23
PMN–0.31 PT	2.585	385.3	3.23
PMN–0.33 PT	2.593	386.1	3.22

profile of PMN-0.38PT single crystal is very similar to the results measured by SE in this work. As the PT content increases, the refractive index of PMN-*x*PT single crystal increases due to the higher refractive index of pure PT as compared to that of pure PMN. The results correspond with the suggestion made by Bing Guo, and Bhalla.[7] The extinction coefficients also decrease and become small when the wavelength is above 500 nm for all measured samples. This indicates that PMN-*x*PT single crystals are transparent in the visible light region, which is consistent with the results by investigating their optical transmission spectra.[15] The sharp increase in *k* signifies a change in the optical properties from dominantly transmission to absorption as the band gap energy is approached. For PMN-*x*PT single crystals, the main contribution of optical loss comes from the band gap as well as domain wall scattering. These mechanisms become increasingly important for photon energies near the band gap.

It is already well known via lattice dynamical theories that the static dielectric behavior of ferroelectrics with BO_6 octahedron building block is determined primarily by the BO_6 octahedra. In the case of optical properties, the BO_6 octahedron assumes special significance since the B-site cation *d* orbits and the O-anion 2*p* orbits associated with each octahedron govern the lower lying conduction bands and the upper valence bands. This lowest energy oscillator is the largest contributor to the dispersion of the refractive index. Other ions in the structure contribute to the higher-lying conduction band and have small effect on the optical properties.[4] From the well known simple dispersion theory, the refractive index can be given by the modified Sellmeier equation in the region of low absorption[8]

$$n^2(\lambda) = A + \frac{B}{\lambda^2 - C} - D \times \lambda^2, \tag{2}$$

where λ is the wavelength in nanometers. With the measured data of the refractive indices, the parameters *A*, *B*, *C*, and *D* can be obtained in terms of least-square fit, as shown in Table I. PMN-*x*PT single crystals are transparent from 400 to 5800 nm,[15] so in the low absorption wavelength range the refractive indices can be calculated by

$$n^2(\lambda) = 5.6875 + \frac{0.0924}{\lambda^2 - 0.0938} - 0.0217 \times \lambda^2 \quad \text{(PMN-0.24PT)}, \tag{3}$$

$$n^2(\lambda) = 5.5957 + \frac{0.1628}{\lambda^2 - 0.0686} + 0.4040 \times \lambda^2 \quad \text{(PMN-0.30PT)}, \tag{4}$$

$$n^2(\lambda) = 6.6344 + \frac{0.0880}{\lambda^2 - 0.0979} - 0.6123 \times \lambda^2 \quad \text{(PMN-0.31PT)}, \tag{5}$$

$$n^2(\lambda) = 5.9302 + \frac{0.2126}{\lambda^2 - 0.0572} + 0.4268 \times \lambda^2 \quad \text{(PMN-0.33PT)}. \tag{6}$$

With these equations, we can calculate the refractive indices of PMN-*x*PT single crystals with the PT contents of 0.24, 0.30, 0.31, and 0.33. In order to compare with other ferroelectrics with ABO_3-type perovskite structure, the refractive indices at the wavelength of 633 nm are calculated and listed in Table II.

The dominating features in the optical properties of PMN-*x*PT single crystals for energies below 3.5 eV come from the interband electronic transitions between the low lying conduction bands and the upper valence bands. Therefore, it is useful to investigate the change in the band gap as the PT content changes. In order to determine the band gap energy, the absorption coefficients α of the single crystals were derived from the extinction coefficients *k* using

$$\alpha = 4\pi k/\lambda. \tag{7}$$

The band gaps of PMN-*x*PT single crystals were then deduced from the absorption coefficient α using the Tauc equation

$$(\alpha h\upsilon)^2 = B(h\upsilon - E_g), \tag{8}$$

where *B* is a constant, E_g is the band gap energy, and $h\upsilon$ is the energy of the incident light. The relation $\alpha \propto \sqrt{h\upsilon - E_g}$ results from the joint density of states. By extrapolating the linear portion of the curve to zero, band gap energies of PMN-*x*PT single crystals can be obtained. An example of PMN-0.24PT single crystal was shown in Fig. 3. The values of E_g with different PT contents are listed in Table II. The results indicate that optical band gap energy of PMN-*x*PT single crystals is a composition-dependent parameter and decreases with PT content.

C. The Sellmeier optical coefficients

Equations (3)–(6) can be used to calculate the refractive indices of PMN-*x*PT single crystals in the wavelength region of 400–5800 nm and they fit the dispersion of the refractive index quite well. However, the parameters *A*, *B*, *C*, and *D* have no special physical significance. An excellent long wavelength approximation, which has the physical signifi-

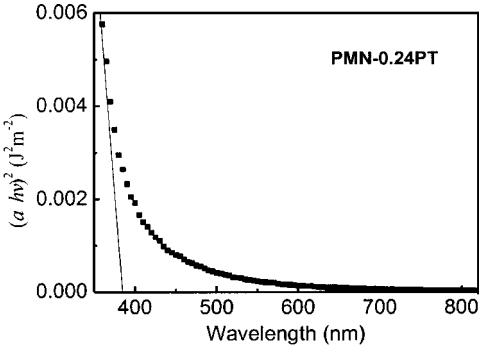

FIG. 3. The dependence of the absorption coefficients $(\alpha hv)^2$ on wavelength for PMN-0.24PT single crystal.

cance of the oscillator parameters, is the single-term Sellmeier relation as shown in following equation:[4,17]

$$n^2 - 1 = \frac{S_0\lambda_0^2}{(1-\lambda_0^2/\lambda^2)} = \frac{E_d E_0}{(E_0^2 - E^2)}, \tag{9}$$

where n is the refractive index at λ and E, which are the wavelength and energy of the incident light, respectively. λ_0 and E_0 are the average oscillator positions and S_0 and E_d are the average oscillator strengths. λ_0 and S_0 can be obtained by plotting $(n^2-1)^{-1}$ versus λ^{-2}, while E_0 and E_d by $(n^2-1)^{-1}$ versus E^2. The dependence of $(n^2-1)^{-1}$ on λ^{-2} and $(n^2-1)^{-1}$ on E^2 for PMN-xPT single crystals are shown in Fig. 4. The parameters are deduced from the slope of the resulting straight fitting lines and from the infinite intercepts. The calculated values of the Sellmeier optical coefficients of PMN-xPT single crystals along with several lead-based compounds with ABO_3-type perovskite structure are listed in Table III. Such parameters are related to the energy gap and energy excitation.[4] For common BO_6-octahedral ferroelectrics, the values of λ_0 and E_0 are very close although the B-site or A-site ions are completely different. S_0 and E_d represent the average strength of interband optical transitions. They are related to the coordination and distribution of cations and anions. These values are more sensitive to the distortion of crystal lattice and the different B-site or A-site ions. As stated above,

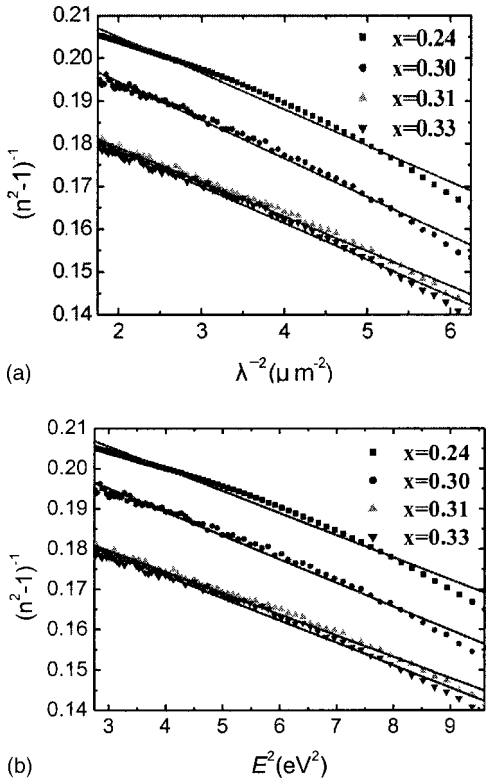

FIG. 4. The dependence of (a) $(n^2-1)^{-1}$ on λ^{-2}, and (b) $(n^2-1)^{-1}$ on E^2 for PMN-xPT single crystals.

PMN-xPT single crystals, like other ABO_3-type perovskite materials, such as PMN, PZN-xPT family, have the common basic BO_6 octahedron building block that determines the basic energy levels in the crystal. The B-site ion has stronger effect on the refined energy level than that of A-site. This determines they have similar values of Sellmeier optical coefficients with a slight difference. In $Pb(B_1B_2)O_3$ ferroelectric relaxors, the nanoregions, domain structure, and order/disorder state of B-site cation structure have influences on the refractive index as well as on the dielectric and piezoelectric behavior of the crystal.[4,7,19] For PMN-xPT single crystals, Mg^{2+}, Nb^{5+}, and Ti^{4+} ions occupy the same crystallographic site in the

TABLE III. The Sellmeier optical parameters of PMN-xPT single crystals and several lead-based materials at 633 nm wavelength at room temperature.

Materials	n	$S_0(\times 10^{14}\ m^{-2})$	$\lambda_0(\mu m)$	E_0(eV)	E_d(eV)	Reference
PMN-0.24PT (single crystal)	2.446	1.109	0.201	6.17	27.63	This work
PMN-0.30PT(single crystal)	2.501	1.124	0.206	6.06	28.52	This work
PMN-0.31PT(single crystal)	2.585	1.208	0.205	6.05	30.70	This work
PMN-0.33PT(single crystal)	2.593	1.170	0.209	5.94	30.31	This work
PMN-0.38PT(single crystal)	2.620 (n_o)	1.004	0.226	5.50	28.10	8,9
	2.601 (n_e)	1.017	0.223	5.57	28.10	8,9
PMN (single crystal)	2.522	1.013	0.216	5.73	27.22	6
PMN-0.30PT(ceramics)	2.598	1.076	0.217	5.71	29.04	7
$PbTiO_3$ (ceramics)	2.668 (n_o)	1.138	0.217	5.71	30.64	10
	2.659 (n_e)	1.067	0.224	5.53	29.66	10
$Pb(Zn_{1/3}Nb_{2/3})O_3$ (PZN) (single crystal)	2.54	1.064	0.214	5.80	28.2	18
PZN-0.04SPT (single crystal)	2.406 (n_o)	0.8	0.227	5.46	22.52	7
	2.356 (n_e)	0.7	0.236	5.25	20.48	7

structure (short- or long-range order states) and the crystal has a complex energy distribution. The distortion of lattice, ion vibration, and interaction of the ions with different directions give rise to complex mechanisms which influence the optical properties of the crystal.

IV. CONCLUSION

The refractive indices and extinction coefficients for PMN-*x*PT single crystals with $x=0.24$, 0.30, 0.31, and 0.33 have been investigated by spectroscopic ellipsometry. Their modified Sellmeier equations of the refractive indices were obtained in terms of least-square fits. The Sellmeier optical coefficients E_0, λ_0, S_0, and E_d were also calculated through fitting the single-term oscillator equation. Modified Sellmeier equations (3)–(6), which involve four parameters, are intrinsically capable of numerically fitting the dispersion of the refractive index to higher accuracy than single-term Sellmeier Eq. (9), which involves only two parameters. However, Eq. (9) is also very useful because it has the physical significance of the oscillator parameters, which is related directly to the energy band structure. The optical band gap energies were also obtained from absorption coefficient spectra. Our results show that as the PT content increases, the refractive index of PMN-*x*PT single crystals increases, while the optical band gap energy decreases. For PMN-*x*PT single crystals, the BO_6 octahedron building blocks are of the most importance since the B-cation *d* orbits and the O-anion 2*p* orbits associated with each octahedron are the major contributors to the energy bands of interest. The optical properties of oxygen-octahedral ferroelectrics are determined primarily by the BO_6 octahedra.

ACKNOWLEDGMENTS

This work is supported by Hong Kong Research Grants Council (Grant No. PolyU 51 93/00P), the Centre for Smart Materials of the Hong Kong Polytechnic University, the National Natural Science Foundation of China (Grant No. 50272075), and the High Technology and Development Project of the People's Republic of China (Grant No. 2002AA325130).

[1]R. F. Service, Science **275**, 1878 (1997).
[2]Z. Yin, H. Luo, P. Wang, and G. Xu, Ferroelectrics **299**, 207 (1999).
[3]S.-E. Park and T. R. Shrout, J. Appl. Phys. **82**, 1804 (1997).
[4]M. DiDomenico, Jr. and S. H. Wemple, J. Appl. Phys. **40**, 720 (1969).
[5]S. H. Wemple and M. DiDomenico, Jr., J. Appl. Phys. **40**, 735 (1969).
[6]D. McHenry, J. Giniewicz, T. Shrout, S. Jang, and A. Bhalla, Ferroelectrics **102**, 160 (1990).
[7]Y. H. Bing, R. Guo, and A. S. Bhalla, Ferroelectrics **242**, 1 (2000).
[8]X. Wan, H. Xu, T. He, D. Lin, and H. Luo, J. Appl. Phys. **93**, 4766 (2003).
[9]X. Wan, T. He, D. Lin, H. Xu, and H. Luo, Acta Phys. Sin. **52**, 2319 (2003).
[10]Landolt-Bomstain, *Ferroelectrics and Related Substances* (Springer, Berlin, 1981) p. 16.
[11]M. Schubert and W. Dollase, Opt. Lett. **27**, 2073 (2002).
[12]H. Tian, W. Luo, A. Ding, J. Choi, C. Lee, and K. No, Thin Solid Films **408**, 200 (2002).
[13]X. Wan, J. Wang, W. L. H. Chan, C. Choy, H. Luo, and Z. Yin, J. Cryst. Growth **263**, 251 (2004).
[14]H. Luo, G. Xu, H. Xu, P. Wang, and Z. Yin, Jpn. J. Appl. Phys., Part 1 **39**, 5581 (2000).
[15]X. Wan, H. Luo, J. Wang, H. L. W. Chan, and C. Choy, Solid State Commun. **129**, 401 (2004).
[16]X. Zhao, B. Fang, H. Cao, Y. Guo, and H. Luo, Mater. Sci. Eng., B **96**, 254 (2002).
[17]J. Brews, Phys. Rev. Lett. **18**, 662 (1967).
[18]G. Burns and F. H. Dacol, Solid State Commun. **48**, 853 (1983).
[19]P. Thacher, J. Appl. Phys. **41**, 4790 (1970).